



RESEARCH ARTICLE

10.1002/2017WR021644

Key Points:

- Extend vertical equilibrium models for slow gravity drainage
- Formulate the model in a multiscale framework
- Maintain the computational efficiency of vertical equilibrium models

Correspondence to:

B. Becker,
beatrix.becker@iws.uni-stuttgart.de

Citation:

Becker, B., Guo, B., Bandilla, K., Celia, M. A., Flemisch, B., & Helmig, R. (2017). A pseudo-vertical equilibrium model for slow gravity drainage dynamics. *Water Resources Research*, 53, 10,491–10,507. <https://doi.org/10.1002/2017WR021644>

Received 4 AUG 2017

Accepted 11 NOV 2017

Accepted article online 20 NOV 2017

Published online 14 DEC 2017

A Pseudo-Vertical Equilibrium Model for Slow Gravity Drainage Dynamics

Beatrix Becker¹ , Bo Guo², Karl Bandilla³ , Michael A. Celia³ , Bernd Flemisch¹ , and Rainer Helmig¹ 

¹Department of Hydromechanics and Modelling of Hydrosystems, University of Stuttgart, Stuttgart, Germany,

²Department of Energy Resources Engineering, Stanford University, Stanford, CA, USA, ³Department of Civil and Environmental Engineering, Princeton University, Princeton, NJ, USA

Abstract Vertical equilibrium (VE) models are computationally efficient and have been widely used for modeling fluid migration in the subsurface. However, they rely on the assumption of instant gravity segregation of the two fluid phases which may not be valid especially for systems that have very slow drainage at low wetting phase saturations. In these cases, the time scale for the wetting phase to reach vertical equilibrium can be several orders of magnitude larger than the time scale of interest, rendering conventional VE models unsuitable. Here we present a pseudo-VE model that relaxes the assumption of instant segregation of the two fluid phases by applying a pseudo-residual saturation inside the plume of the injected fluid that declines over time due to slow vertical drainage. This pseudo-VE model is cast in a multiscale framework for vertically integrated models with the vertical drainage solved as a fine-scale problem. Two types of fine-scale models are developed for the vertical drainage, which lead to two pseudo-VE models. Comparisons with a conventional VE model and a full multidimensional model show that the pseudo-VE models have much wider applicability than the conventional VE model while maintaining the computational benefit of the conventional VE model.

1. Introduction

Storage of gas in the deep subsurface is increasingly important in many energy related applications. For almost 100 years, seasonal storage of natural gas in the subsurface has contributed to the reliability of energy supply. In the past decades, large-scale geological storage of CO₂ has been identified as a promising technology to reduce carbon emissions to mitigate global warming (Celia et al., 2015; Metz et al., 2005). More recent research efforts concentrate on using the subsurface to compensate daily to weekly fluctuations in the energy output of intermittent renewable energy sources. This is done, e.g., by using excess energy to compress air (Oldenburg & Pan, 2013) or to produce hydrogen via hydrolysis (Mignard et al., 2016; Pfeiffer et al., 2017), with the gas stored in the subsurface and then extracted to generate energy at a later time.

Deep saline aquifers are often convenient targets for gas storage. When gas (e.g., CO₂ or CH₄) is injected into a saline aquifer, it forms a two-phase flow system in which gas displaces the resident brine and moves laterally outward from the injection point. At the same time, the injected gas tends to move upward because of the large density contrast between gas and brine. Modeling the migration of gas in the saline aquifer is critical to ensure long-term security of underground gas storage, as well as to determine financial costs and optimal operational parameters. Gas storage in the subsurface often involves large spatial and temporal scales that lead to high computational cost for modeling the gas migration. Additionally, accuracy of the models often requires very fine grid resolutions in order to reliably capture the caprock geometry in lateral direction and the thin gas layer in the vertical direction, leading to prohibitive computational costs. In addition, a large number of simulation runs may need to be done to quantify parameter uncertainty in the subsurface (e.g., Monte Carlo simulation) further exacerbating the computational demand. Accordingly, for these simulations, computationally inexpensive tools are required.

A group of simplified models can be developed by assuming vertical equilibrium (VE) of the two fluid phases (Lake, 1989; Yortsos, 1995). Such a vertical equilibrium assumption allows elimination of the vertical

dimension by vertical integration of the three-dimensional governing equations, which significantly reduces the computational cost. Analytical solutions to gravity-segregated flow have been developed assuming lateral symmetry for unconfined aquifers (Golding et al., 2011; Huppert & Woods, 1995; Lyle et al., 2005) and for confined aquifers (Dentz & Tartakovsky, 2009; Guo et al., 2016; Hesse et al., 2007; Juanes et al., 2010; Nordbotten & Celia, 2006; Pegler et al., 2014; Zheng et al., 2015) with later works primarily focused on CO₂ sequestration. VE models have to be solved numerically if capillary pressure or heterogeneities are included. These numerical VE models rely on integrated equations with numerically upscaled parameters depending on the phase distribution in the vertical extent (Nordbotten & Celia, 2011).

VE models have been applied to field-scale applications (Bandilla & Celia, 2017; Bandilla et al., 2012, 2014; Gasda et al., 2012; Nilsen et al., 2011; Person et al., 2010) and benchmark exercises (Class et al., 2009; Nordbotten et al., 2012). For certain injection conditions, VE models have been found to be even more accurate than conventional 3-D simulations (Ligaarden & Nilsen, 2010). The applicability of VE models is discussed in Court et al. (2012) and Nordbotten and Celia (2011) with regard to temporal and spatial scales. For the VE assumption to hold, the brine and gaseous phase need to segregate until a hydrostatic pressure profile in the vertical direction is reached. The time scale for segregation of the two fluid phases in the vertical direction needs to be short relative to the time scale of interest, and varies depending on geological parameters and the properties of the fluid. The permeability in the vertical direction plays an especially important role, with larger permeabilities leading to shorter segregation times.

For some cases, the time until the VE assumption is valid can be much longer than the time scales of interest, even if the permeability in the vertical direction is large. For nonlinear relative permeability functions, like the commonly used Brooks-Corey power law, the relative permeability of the wetting phase approaches zero during the drainage process, leading to a slow-down of the drainage with time. Such slow drainage may be captured by solving a subscale problem in the vertical direction in a vertically integrated framework introduced by Nordbotten and Celia (2011). In this framework, the vertically integrated equations correspond to the coarse scale while the underlying saturation profile in the vertical direction is the fine scale. In the case of conventional VE models, the fine-scale solution is solved analytically using the VE assumption. Guo et al. (2014) extended this multiscale framework and developed a vertically integrated model that does not rely on the VE assumption. This is done by solving one-dimensional vertical flow dynamics as fine-scale problems for each of the coarse-scale numerical grid cells at every time step. However, the dynamic computations in the vertical direction come with a slightly higher computational demand than conventional VE models.

In this paper, we take this multiscale framework and extend the VE model to capture slow gravity drainage due to relative permeability functions with large exponents. We develop a pseudo-VE model that assumes that due to the slow drainage a vertically uniform pseudo-residual saturation exists within the plume that is larger than the ultimate (long-time) residual saturation and decreases with time. The model solves vertically integrated equations on the coarse scale and analytically solves the slow gravity drainage as a fine-scale problem, thereby reducing the pseudo-residual saturation dynamically in each time step. The two scales are coupled sequentially. We present two versions of the pseudo-VE model, where the first version assumes a single pseudo-residual saturation inside the entire plume and the second version assumes varying pseudo-residual saturations along the horizontal direction of the plume. We refer to these models as pseudo-VE models in the sense that we assume they are in vertical equilibrium at every time step with a pseudo-residual saturation that is determined explicitly and continuously updated. The pseudo-VE models have a much broader applicability compared to the conventional VE models and fully maintain the low computational cost.

We first give a review of the conventional VE model and the VE assumption, which is followed by introduction of the pseudo-vertical equilibrium concept and the multiscale framework for VE models. Then we present the two newly developed versions of the pseudo-VE model and apply them to different gas injection scenarios. Finally, we show comparisons of the pseudo-VE models, the conventional VE model, and the full multidimensional model to demonstrate the applicabilities of the new pseudo-VE models.

2. Vertical Equilibrium Model

In this section, we first present the three-dimensional governing equations for two-phase flow in a porous medium and in a second step, we derive the coarse-scale and fine-scale equations for the VE model by

integrating the three-dimensional governing equations in the vertical direction (denoted as z-direction). We refer to vertically integrated variables as “coarse-scale” variables, denoted by upper case letters, while the variations along the vertical are “fine-scale” variables and will be denoted by lower case letters.

2.1. Three-Dimensional Governing Equations

The three-dimensional mass balance for each fluid phase α , assuming incompressible fluid phases and a rigid solid matrix, is

$$\phi \frac{\partial s_\alpha}{\partial t} + \nabla \cdot \mathbf{u}_\alpha = q_\alpha, \quad \alpha = w, n, \tag{1}$$

where ϕ is the porosity, s_α the phase saturation, t the time [T], \mathbf{u}_α the Darcy flux [L/T], and q_α the source/sink term [1/T]. The phase α can either be a wetting phase “w” or be a nonwetting phase “n”, resulting in two mass balance equations that need to be solved for a two-phase system. The assumption of incompressible fluid phases is done here for simplicity of presentation.

The extension of Darcy’s law for multiphase flow states for each phase α that

$$\mathbf{u}_\alpha = -\mathbf{k} \frac{k_{r,\alpha}}{\mu_\alpha} (\nabla p_\alpha + \rho_\alpha g \nabla z), \quad \alpha = w, n, \tag{2}$$

where \mathbf{k} is the intrinsic permeability tensor [L²], $k_{r,\alpha}$ is the relative permeability of a phase α which depends on the wetting phase saturation s_w and has to be determined empirically, μ_α is the viscosity [M/(L T)] of phase α , p_α is the pressure [M/(L T²)] of phase α , ρ_α is the density [M/L³] of phase α , g is the gravitational acceleration [L/T²], and z is the vertical coordinate [L]. Introducing the phase mobility λ_α [(L T)/M] of a phase α with $\lambda_\alpha = \frac{k_{r,\alpha}}{\mu_\alpha}$, equation (2) can be written as

$$\mathbf{u}_\alpha = -\mathbf{k} \lambda_\alpha (\nabla p_\alpha + \rho_\alpha g \nabla z), \quad \alpha = w, n. \tag{3}$$

The two equations (one for each phase) resulting from (1) with Darcy’s law (3) inserted can be solved for the four primary unknowns, p_α and s_α , by using the closure equations $s_w + s_n = 1$ and $p_c(s_w) = p_n - p_w$, where $p_c(s_w)$ is the capillary pressure, which is assumed to be a function of wetting phase saturation s_w .

2.2. Coarse-Scale and Fine-Scale Equations of VE Model

The VE assumption postulates that the two fluid phases have segregated due to buoyancy (i.e., no more vertical flow), and that the phase pressures have reached gravity-capillary equilibrium in the vertical direction. With the VE assumption, the form of the pressure distribution is known, a priori, in the vertical direction. This can be used to simplify the governing equations of fluid flow and leads naturally to vertical integration of the governing equations with associated reduction of dimensionality. The details along the vertical direction can be reconstructed from the imposed equilibrium pressure distribution.

In the following we assume that the nonwetting phase (e.g., gas) is less dense than the wetting phase (e.g., brine) and that the nonwetting phase consequently forms a plume below a no-flow upper boundary. For simplicity of presentation, we assume an aquifer with impermeable top and bottom. The mass balance equation (1) is integrated over the vertical direction from the bottom of the aquifer, ζ_B , to the top of the aquifer, ζ_T , to derive the coarse-scale equations for the VE model:

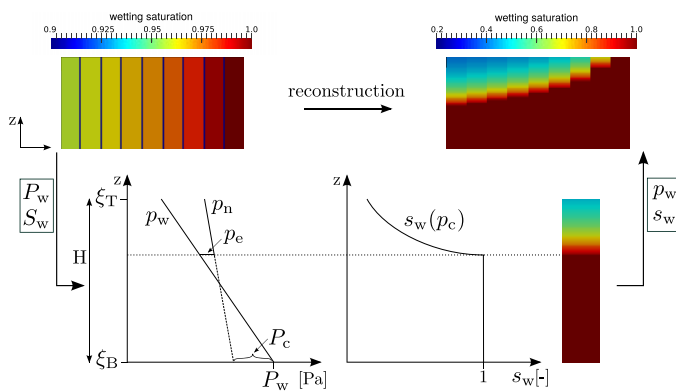
$$\int_{\zeta_B}^{\zeta_T} \phi \frac{\partial s_\alpha}{\partial t} dz + \int_{\zeta_B}^{\zeta_T} \nabla \cdot \mathbf{u}_\alpha dz = \int_{\zeta_B}^{\zeta_T} q_\alpha dz, \quad \alpha = w, n. \tag{4}$$

We introduce the depth-integrated parameters:

$$\Phi = \int_{\zeta_B}^{\zeta_T} \phi dz, \tag{5}$$

$$S_\alpha = \frac{1}{\Phi} \int_{\zeta_B}^{\zeta_T} \phi s_\alpha dz, \tag{6}$$

$$\mathbf{U}_\alpha = \int_{\zeta_B}^{\zeta_T} \mathbf{u}_{\alpha, //} dz, \tag{7}$$



$$Q_\alpha = \int_{\xi_B}^{\xi_T} q_\alpha dz, \quad (8)$$

with the subscript “//” denoting the xy -plane. This results in the depth-integrated equations:

$$\Phi \frac{\partial S_\alpha}{\partial t} + \nabla_{//} \cdot \mathbf{U}_\alpha = Q_\alpha, \quad \alpha = w, n. \quad (9)$$

The depth-integrated Darcy flux is found by vertically integrating Darcy’s law over the height of the aquifer as

$$\mathbf{U}_\alpha = -\mathbf{K} \Lambda_\alpha (\nabla_{//} P_\alpha + \rho_\alpha g \nabla_{//} \xi_B), \quad \alpha = w, n, \quad (10)$$

with the depth-integrated permeability and depth-averaged mobility:

$$\mathbf{K} = \int_{\xi_B}^{\xi_T} \mathbf{k}_{//} dz, \quad (11)$$

$$\Lambda_\alpha = \mathbf{K}^{-1} \int_{\xi_B}^{\xi_T} \mathbf{k}_{//} \lambda_\alpha dz. \quad (12)$$

Figure 1. Reconstruction of (top right) the fine-scale solution in the vertical direction based on (top left) the computed coarse-scale solution. (bottom left) The assumption of vertical equilibrium leads to hydrostatic pressure profiles for wetting and nonwetting phase, which can be constructed based on the coarse-scale wetting phase pressure P_w and coarse-scale pseudo-capillary pressure P_c at the bottom of the aquifer. (bottom right) The wetting phase saturation profile in the vertical direction results from the inverse of the fine-scale capillary pressure function.

The coarse-scale pressure P_α of phase α in the vertically integrated Darcy’s law is defined as the phase pressure at the bottom of the aquifer.

Two closure equations are required again to solve for the four unknown primary variables P_α and S_α : $S_w + S_n = 1$ and the coarse-scale pseudo-capillary pressure $P_c(S_w) = P_n - P_w$ that relates the coarse-scale pressure difference at the bottom of the aquifer to the coarse-scale saturation. The coarse-scale nonwetting phase pressure at the bottom of the aquifer P_n is constructed from the linear extension of the pressure distribution for the nonwetting phase inside the plume to regions below that. We solve the coarse-scale equation (9) with the depth-integrated Darcy flux (10) inserted. After the coarse-scale problem is solved, the fine-scale solution in the vertical direction can be reconstructed based on the coarse-scale quantities P_α and S_α (see Figure 1). The fine-scale pressure is reconstructed based on the above stated assumption of a hydrostatic pressure profile. Given the two fine-scale phase pressures at every point in the vertical direction, the fine-scale capillary pressure function $p_c(s_w)$ can be inverted to give the fine-scale saturation profile. The fine-scale saturation is used to calculate the fine-scale relative permeability. By integrating the fine-scale relative permeability using equation (12), the coarse-scale relative permeability can be updated.

3. Pseudo-Vertical Equilibrium and Multiscale Framework

The time scale associated with gravity segregation of the two fluid phases generally depends on physical parameters such as the permeability in the vertical direction, the density difference of the fluids and the height of the confined aquifer (Ewing et al., 2015; Hunt et al., 2013; Nordbotten & Dahle, 2011). The shape of the relative permeability function can also play a significant role. Commonly used are power functions like the Brooks-Corey law:

$$k_{r,w} = \left(\frac{s_w - s_{wr}}{1 - s_{wr} - s_{nr}} \right)^{(2/\lambda+3)} = s_{we}^{(2/\lambda+3)}, \quad k_{r,n} = (1 - s_{we})^2 \left(1 - s_{we}^{(2/\lambda+1)} \right), \quad (13)$$

where s_{wr} and s_{nr} are residual wetting and nonwetting phase saturations respectively and s_{we} is the effective wetting phase saturation. As the displaced fluid (oftentimes the wetting phase) drains out from the plume of injected fluid due to gravity, the saturation of the wetting phase in the plume of the injected fluid decreases. For nonlinear relative permeability-saturation relationships like the Brooks-Corey law, relative permeability is very low for small to medium wetting phase saturations and high only for larger saturations (see Figure 2 for examples of relative permeability-saturation relationships with different parameters). At the same time the driving force (density difference) stays the same. With that, a relative permeability and thus a mobility close to zero means that the flux of the wetting phase draining out of the plume decays rapidly as the wetting phase saturation decreases toward its residual value. Because of this large power law nonlinearity of the relative

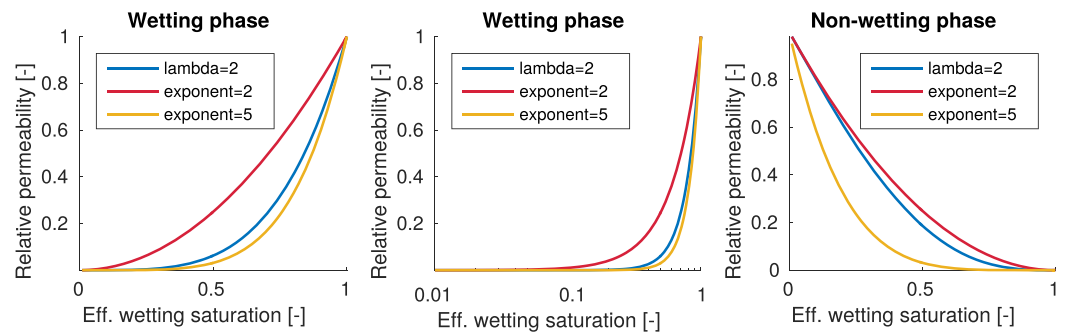


Figure 2. Relative permeability as a function of wetting phase saturation, for the wetting phase (linear and logarithmic scale) and nonwetting phase. Shown is the Brooks-Corey law with $\lambda = 2$ and a power function with exponents 2 and 5 of the form $k_{r,w} = s_{we}^{\text{exp}}$, $k_{r,n} = (1 - s_{we})^{\text{exp}}$. See Court et al. (2012) for ranges of parameters in relative permeability functions.

permeability, the segregation time can be very long, with the saturation of the wetting phase not reaching its residual saturation even after hundreds to thousands of years, even if the permeability in the vertical direction is large. In those cases, the nonwetting phase plume appears to be in equilibrium, in the sense that the wetting phase saturation inside the plume stays almost constant over a long period of time although it is still above the ultimate residual saturation and the nonwetting phase is very close to vertical equilibrium. We refer to this type of fluid distribution as pseudo-equilibrium.

Conventional VE models do not reflect the slow-down of drainage and assume instant gravity segregation of both phases from the beginning of the simulation. This can lead to inaccurate results, especially for relative permeability functions with large exponents. Figure 3 shows the gas distribution after 4.5 years of gas injection for a case with a relative permeability function with a large exponent (case 1 in Table 1). It shows clearly that the full multidimensional reference solution is not reproduced by the conventional VE model even though it appears that gravity segregation has occurred and the fluids are close to vertical equilibrium. The full multidimensional reference solution shows a wetting phase saturation inside the gas plume that is larger than the ultimate residual saturation, indicating that full segregation has not taken place yet. This wetting phase saturation inside the plume acts like a residual saturation because the relative permeability is

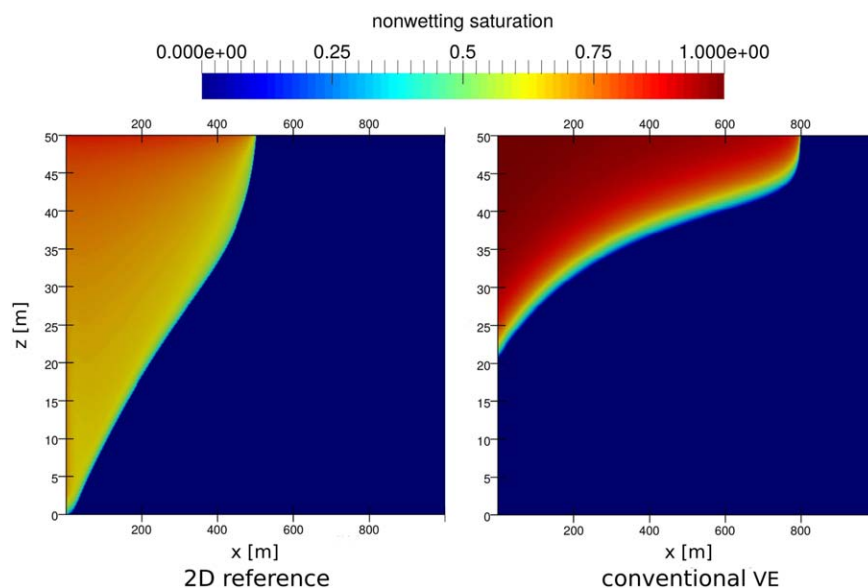


Figure 3. Gas injection into a brine-filled confined aquifer with a relative permeability function with large exponent (exponent 5). Shown is the gas plume after 4.5 years (left) for the full multidimensional model and (right) for the conventional VE model. Parameters for the simulation are taken from case 1 in Table 1.

Table 1
Parameter Combinations Considered in the Simulations

Cases	Porosity	Permeability horizontal (mD)	Permeability vertical (mD)	B.C. λ for p_c	Entry pressure (Pa)	Inflow rate (kg/(s m))	Aquifer height (m)
1	0.15	100	100	2	1×10^4	7.1×10^{-3}	50
2	0.15	100	100	2	5×10^4	7.1×10^{-3}	50
3	0.15	100	100	2	1.5×10^4	7.1×10^{-3}	50
4	0.15	66.6	66.6	2	1×10^4	7.1×10^{-3}	50
5	0.15	1,000	1,000	2	1×10^4	7.1×10^{-3}	50
6	0.15	100	100	2	1×10^4	2.37×10^{-3}	50
7	0.15	100	100	2	1×10^4	8.9×10^{-3}	50
8	0.2	100	100	2	1×10^4	7.1×10^{-3}	50
9	0.3	100	100	2	1×10^4	7.1×10^{-3}	50
10	0.15	100	100	2	1×10^4	7.1×10^{-3}	30
11	0.15	100	100	2	1×10^4	7.1×10^{-3}	60
12	0.15	100	100	1.5	1×10^4	7.1×10^{-3}	50
13	0.15	100	100	2.5	1×10^4	7.1×10^{-3}	50
14	0.15	50	100	2.5	1×10^4	7.1×10^{-3}	50
15	0.15	100	100	2.5	3×10^4	7.5×10^{-4}	50

almost zero at this value, which is why we refer to it as pseudo-residual saturation. The conventional VE model assumes instant gravity segregation of the two fluid phases, which leads to different saturation profiles in the vertical direction for the conventional VE model and the full multidimensional model. In the case of nonlinear relative permeability functions, the fine-scale saturation profiles and thus the distribution of the relative permeability in the vertical direction has a direct influence on the conventional VE model. As a result, incorrect representation of the saturation profiles in the vertical direction leads to incorrect prediction of the plume development.

To extend VE models to capture slow gravity drainage due to relative permeability functions with large exponents, we take the multiscale framework from Nordbotten and Celia (2011), extended by Guo et al. (2014), and develop a so-called pseudo-VE model. The pseudo-VE model involves a coarse scale which is identical to the coarse scale of conventional VE models and a fine scale where simple gravity drainage is considered. In the reconstruction step we apply a uniform pseudo-residual wetting phase saturation inside the plume which is larger than the ultimate residual saturation of the wetting phase. This

way, the pseudo-VE model accounts for the pseudo-segregated state of the two fluid phases that can be observed for cases with relative permeability functions with large exponents. A larger residual wetting phase saturation was used by Swickrath et al. (2016) as well, leading to improved results compared to full multidimensional models. However, their residual wetting phase saturation is constant in both space and time and has to be fitted by running a full multidimensional model. In our model the pseudo-residual saturation is an analytical function derived using physical arguments, and it is dynamically updated during the simulation at every time step after solving the coarse-scale VE model. This leads to much broader applicability.

We point out that, in terms of complexity, the pseudo-VE model is an intermediate model in between the conventional VE model and the dynamic reconstruction model from Guo et al. (2014). Compared to conventional VE models, the additional computation in the pseudo-VE model is a simple algebraic calculation and therefore we expect the pseudo-VE model to be computationally as fast as conventional VE models.

4. Pseudo-VE Model

We propose a pseudo-VE model that accounts for the effect of slow drainage due to large exponents in the relative permeability-saturation function during the reconstruction step. Instead of assuming residual wetting phase saturation inside the plume from the first time step on, the pseudo-VE model uses an explicit approximation for a pseudo-residual saturation s_{wr}^* inside the plume which dynamically approaches the ultimate residual wetting phase saturation as time increases. By doing this, we relax the assumption of instant gravity segregation.

In the following, we describe the algorithm for the pseudo-VE model. Then we give an approximation of the pseudo-residual saturation. Lastly, we present two versions of the pseudo-VE model with varying complexities in the conceptual approach and expected accuracy of the model: the global pseudo-VE model uses a globally constant pseudo-residual saturation inside the plume while the local pseudo-VE model regards the drainage process within each vertical grid column by calculating separate pseudo-residual saturations along the horizontal direction.

4.1. Algorithm of the Pseudo-VE Model

By casting the pseudo-VE model into the multiscale framework we can identify two scales that are solved sequentially. On the coarse scale, the vertically integrated equations of the VE model (9) with the depth-integrated Darcy flux (10) inserted are solved using an IMPES time discretization and a cell-centered finite-volume method for discretization in space. The time stepping criterion is based on a Courant-Friedrichs-Lewis (CFL) condition (Courant et al., 1928). The fine scale is a simple model to capture the slow gravity

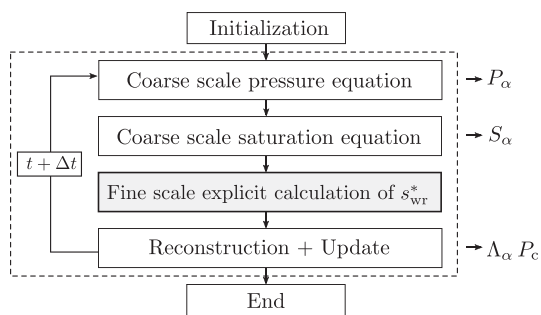


Figure 4. IMPES algorithm for the pseudo-VE model solving incompressible iso-thermal multiphase flow.

drainage that updates the residual saturation. It is this simple model that forms the basis of the pseudo-VE approach.

The algorithm of the pseudo-VE model is summarized in Figure 4. As a first step in the algorithm, an IMPES calculation on the coarse scale is performed. This results in the primary variables on the coarse scale, P_α and S_α , computed at the new discrete time level. Then the fine scale with the drainage process in the vertical direction is taken into account and the pseudo-residual saturation inside the plume is updated. This step is followed by the reconstruction of the fine-scale variables, where the updated pseudo-residual saturation inside the plume and the primary variables are used to reconstruct the solution in the vertical direction. Based on the saturation profile in the vertical

direction, the integrated coarse-scale relative permeability and coarse-scale capillary pressure are determined. These coarse-scale quantities are then applied for the next IMPES time step on the coarse scale. Following this algorithm, the pseudo-VE model preserves the low computational cost of the VE model since the explicit calculations of the vertical drainage add very little additional computational effort. We note that we can also solve the pseudo-VE model with a fully implicit time-stepping scheme. Such fully implicit time-stepping will require more computational effort for each time step due to the larger set of unknowns (e.g., vertical drainage state in addition to the usual pressure and saturation variables).

We note that the pseudo-residual wetting phase saturation is only used to modify the fine-scale saturation profile. All constitutive relationships depending on saturation (e.g., fine-scale relative permeability-saturation relationship) are not altered and effective saturations to evaluate those relationships are calculated based on the ultimate residual saturation. Thus, the difference of the pseudo-VE model to the conventional VE model solely lies in the reconstructed fine-scale saturation profile. This profile in turn directly affects the value of the coarse-scale relative permeability and coarse-scale capillary pressure, and thus the evolution of the entire plume.

4.2. Explicit Update of the Pseudo-Residual Saturation on the Fine Scale

The pseudo-residual wetting phase saturation inside the plume is determined by computing the drainage flux of the wetting phase out of the plume after each IMPES time step on the coarse scale. To illustrate the approach, we consider a closed vertical column with a plume height h_i [L] and a pseudo-residual saturation $s_{wr,i}^*$ inside the plume. If capillary forces are present, the time scale to reach vertical equilibrium is smaller since the wetting phase saturation does not need to reach low saturation values everywhere inside the plume. For cases with nonzero fine-scale capillary pressure, we define the capillary transition zone (CTZ) as the region of the plume where the wetting phase saturation is significantly above residual. Following Court et al. (2012) and Lake (1989), we define the thickness of the transition zone as

$$CTZ = \frac{p_e - p_c(s_{10\%})}{(\rho_w - \rho_n)g}, \tag{14}$$

with the entry pressure p_e [$M/(L T^2)$] being the capillary pressure at a saturation of $s_w = 1.0$, and $p_c(s_{10\%})$ [$M/(L T^2)$] being the capillary pressure at a 10% threshold saturation $s_{10\%} = s_{wr} + 0.1(1.0 - s_{wr})$. In our simplified model for the pseudo-residual saturation, we assume that within the CTZ the wetting phase has reached vertical equilibrium. In the following, the nonwetting phase plume height h in the case of capillary pressure always excludes the CTZ from the full plume height h_{tot} :

$$h = \begin{cases} h_{tot} - CTZ & \text{for } h_{tot} > CTZ, \\ 0 & \text{for } h_{tot} \leq CTZ. \end{cases} \tag{15}$$

During a time step Δt the wetting phase drains out of the plume, which leads to a decrease of the plume height h_i and a decrease of the pseudo-residual saturation inside the plume. Because of the nonlinear relative permeability functions, gravity drainage in the vertical direction would typically lead to the formation of a shock followed by a rarefaction wave. For simplicity, we assume a constant pseudo-residual saturation $s_{wr,i}^*$ inside the plume during Δt .

The Darcy flux of wetting phase draining out of the plume can be approximated based on the total Darcy flux $u_{tot} = u_w + u_n$ [L/T] and fractional flow function $f_w = \lambda_w / (\lambda_w + \lambda_n)$ as

$$u_w = f_w u_{tot} + \lambda_n f_w k (g \nabla z (\rho_n - \rho_w) + \nabla p_c). \quad (16)$$

If a one-dimensional vertical column is considered that is closed at the top and the bottom, the total Darcy flux u_{tot} equals zero. This implies countercurrent flow where the nonwetting phase moves from the bottom to the top and the wetting phase from the top to the bottom. Thus, with $\frac{\partial z}{\partial z} = -1$ against the z -direction, the Darcy flux of the wetting phase out of the plume is given as

$$u_{w,z} = \lambda_n f_w k \left(g (\rho_w - \rho_n) + \frac{\partial p_c}{\partial z} \right). \quad (17)$$

When capillary forces are neglected, we have the following approximation of the Darcy flux for the segregation process:

$$u_{w,z} \approx \lambda_n f_w k g (\rho_w - \rho_n). \quad (18)$$

With the assumption of a constant pseudo-residual saturation during Δt the nonwetting phase mobility λ_n and the fractional flow function f_w are evaluated based on the pseudo-residual saturation $s_{wr,i}^*$. The updated plume height h_{i+1} follows as

$$h_{i+1} = h_i - \frac{u_{w,z} \Delta t}{\phi (1 - s_{wr,i}^*)}. \quad (19)$$

The mass balance for the wetting phase inside the column is

$$(H - h_i) \phi + h_i \phi s_{wr,i}^* = (H - h_{i+1}) \phi + h_{i+1} \phi s_{wr,i+1}^*. \quad (20)$$

Finally, the updated pseudo-residual saturation $s_{wr,i+1}^*$ can be obtained by rearranging (20) and inserting (19):

$$s_{wr,i+1}^* = \frac{h_i \phi s_{wr,i}^* - \frac{u_{w,z} \Delta t}{(1 - s_{wr,i}^*)}}{h_i \phi - \frac{u_{w,z} \Delta t}{(1 - s_{wr,i}^*)}}. \quad (21)$$

The wetting phase saturation is assumed to be constant within the plume during vertical drainage. This leads to faster drainage because the drainage velocity decreases with saturation. The explicit calculation of the pseudo-residual saturation therefore requires a time step restriction for the segregation process. The wetting phase that drains out of the plume in one time step cannot exceed the amount of wetting phase that is inside the plume. Following this, the time step is limited due to the explicit calculation of the pseudo-residual saturation by

$$\Delta t \leq \frac{h_i \phi s_{wr,i}^* (1 - s_{wr,i}^*)}{u_{w,z}}. \quad (22)$$

It is expected that the time step limitation due to the pseudo-residual saturation update plays a role mostly during early times of the simulation. In the beginning of the segregation process the velocities in the vertical direction will be large and the time stepping will be limited by (22). With time, the segregation process slows down as the wetting phase saturation inside the plume decreases. Accordingly, for later times the CFL-criterion from the coarse-scale simulation (horizontal flow) will be more restrictive.

4.3. Global and Local Pseudo-VE Model

The pseudo-residual wetting phase saturation can either be determined for the entire plume (referred to as global pseudo-VE model) or for each vertical column inside the plume separately (referred to as local pseudo-VE model). For the global pseudo-VE model, a total drainage flux out of the plume is computed, which leads to a single value for the pseudo-residual saturation that is valid for the entire plume. For the local pseudo-VE model, we calculate the drainage flux out of each vertical column in the plume, leading to a separate pseudo-residual saturation for each column.

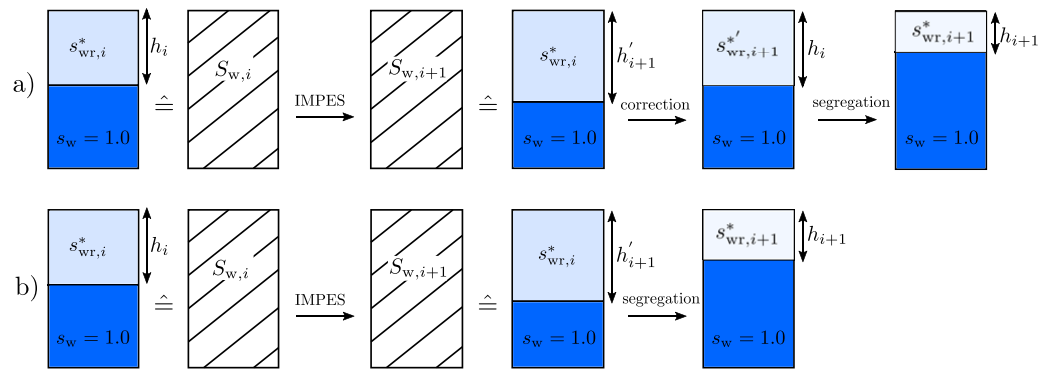


Figure 5. Sequence of calculation of the pseudo-residual wetting phase saturation. (a) Global pseudo-VE model and (b) local pseudo-VE model.

In the *global pseudo-VE model* we consider an averaged plume during the drainage calculation on the fine scale. The entire plume height is averaged over its horizontal length, resulting in an averaged nonwetting phase plume height h . For the case that capillary pressure is included, the gas plume height h follows from averaging the plume height above the CTZ for all vertical columns. As a result of averaging the plume, we observed a slower decrease of the pseudo-residual saturation compared to the full multidimensional model. Accordingly, we suggest to enhance the segregation process by applying a correction to the global pseudo-VE model. This correction is based on the assumption that the averaged height of the plume and the CTZ of the entire plume are constant during the coarse-scale IMPES step and only changes afterward due to segregation. If the plume does not advance in one time step, this implies that nonwetting phase entering the plume at the injection well replaces the wetting phase inside the plume instead of adding to the averaged height of the plume. Such correction gives the best results based on our observations.

In the following, we present the sequence of the fine-scale calculations for the global pseudo-VE model as illustrated in Figure 5a). During the coarse-scale time step the averaged coarse-scale saturation inside the columns of the plume changes from $S_{w,i}$ to $S_{w,i+1}$. After the coarse-scale time step, the correction step leads to an update of the pseudo-residual saturation, so that $h'_{i+1} = h_i$:

$$s_{wr,i+1}^{*f} = s_{wr,i}^* + \frac{(S_{w,i+1} - S_{w,i})H}{(H - h_i)} \quad (23)$$

Following this, gravity drainage of the wetting phase is computed based on (21), with the adjusted gas plume height h_i and the adjusted pseudo-residual saturation $s_{wr,i+1}^{*f}$. This leads to the final pseudo-residual saturation:

$$s_{wr,i+1}^* = \frac{h_i \phi s_{wr,i+1}^{*f} - \frac{u_{wz} \Delta t}{(1 - s_{wr,i+1}^{*f})}}{h_i \phi - \frac{u_{wz} \Delta t}{(1 - s_{wr,i+1}^{*f})}} \quad (24)$$

with the flux of the wetting phase draining out of the plume based on $s_{wr,i}^*$.

In the *local pseudo-VE model*, the pseudo-residual saturation is updated for each vertical grid column, without averaging the gas plume height. Differences in the plume height along the horizontal direction are thus directly included by considering each column separately and the correction of the gas plume height due to effects of averaging are not necessary. The sequence of the calculation for the local pseudo-VE model is illustrated in Figure 5b). The drainage flux is calculated using equation (21), with the plume height h'_{i+1} and a flux of the wetting phase draining out of the plume that is based on $s_{wr,i}^*$ as before. This results in an update for the pseudo-residual saturation in each column:

$$s_{wr,i+1}^* = \frac{h'_{i+1} \phi s_{wr,i}^* - \frac{u_{wz} \Delta t}{(1 - s_{wr,i}^*)}}{h'_{i+1} \phi - \frac{u_{wz} \Delta t}{(1 - s_{wr,i}^*)}} \quad (25)$$

In contrast to the global pseudo-VE model, additional considerations need to be taken into account for columns that have not been entered by the plume previously and thus have an unknown initial pseudo-residual saturation. These columns get assigned an initial pseudo-residual saturation that is equal to the average pseudo-residual saturation over all columns inside the plume. We consider the average pseudo-residual saturation in the plume a characteristic value for the system. Using it as the initial pseudo-residual saturation for the leading edge gives best results in our simulations. This is also done as a correction for a column when the time step restriction (22) is violated.

5. Results and Discussion

We show accuracy, robustness and efficiency for both pseudo-VE models by comparing the solutions against a conventional VE model and a full multidimensional model. The pseudo-VE models, the conventional VE model and the full multidimensional model are all implemented in DuMu^x (Ackermann et al., 2017; Flemisch et al., 2011).

We design 15 base test cases (see Table 1) of gas injection into an aquifer filled with brine to analyze:

1. dynamic migration of the gas front with the change of the inflow rate,
2. anisotropy of the aquifer and influence on the segregation process,
3. influence of capillarity and especially entry pressure, and
4. behavior for different viscosity and density ratios,

for different realistic aquifer parameters. We show the influence of the power law nonlinearity of the relative permeability function by applying three different relative permeability-saturation relationships to every base test case. This leads to 45 different cases in total. The three relative permeability functions that we use are power functions with exponents 2 and 5 and a Brooks-Corey relationship with $\lambda = 2$, as shown in Figure 2. The Brooks-Corey relationship with the chosen parameter $\lambda = 2$ results in a relative permeability function for the gas phase that is similar to the power law with an exponent 2. For the brine phase this Brooks-Corey relationship results in a function that is close to a case of exponent 5. We consider the Brooks-Corey relationship a mixed case in terms of power law nonlinearity of the relative permeability functions.

For simplicity, we solve the injection scenarios in two dimensions (horizontal and vertical). However, this is not a necessity for the newly developed pseudo-VE algorithm. In each test case we inject supercritical CO₂ (supercritical CH₄ in case 15) over the entire depth of one side of a two-dimensional homogeneous domain whose pore space is filled with brine. The other side is open for flow (Dirichlet boundary condition) and sufficiently far away from the injection that no gas crosses the boundary. On the open side we fix the brine phase saturation to $s_w = 1.0$ and prescribe a hydrostatic distribution of the brine phase pressure p_w , starting with 1.0×10^7 Pa at the top. The top and bottom of the domain are closed. We assume a density of CO₂ of 710 kg/m^3 and a viscosity of CO₂ of 4.25×10^{-5} Pa s. For case 15, we assume a density of CH₄ of 59.2 kg/m^3 and a viscosity of CH₄ of 1.202×10^{-5} Pa s. The density of the brine phase is assumed to be 991 kg/m^3 and the viscosity of the brine phase 5.23×10^{-4} Pa s. The residual saturations of both phases are assumed to be zero.

We use a full multidimensional model as a reference to compare with our pseudo-VE models. We performed a grid convergence test to ensure a converged solution on our two-dimensional grid. Based on that, a resolution of the grid of 2 m in the horizontal direction and 0.125 m in the vertical direction was chosen to generate the two-dimensional reference solutions of all test cases in Table 1 with the relative permeability-saturation relationships from Figure 2. Following that, all test cases were simulated with the three VE models: the global pseudo-VE model, the local pseudo-VE model and the conventional VE model. The same resolution in the horizontal direction was chosen as for the reference solutions. For all our test cases, the two pseudo-VE models are similar to the conventional VE model in terms of computational time, and three orders of magnitude faster than the reference model.

We note that the time step restriction due to vertical segregation as in equation (22) has been in none of the cases for the global pseudo-VE model more restrictive than the CFL-condition applied for the coarse-scale simulation. In the global pseudo-VE model the columns with small plume heights are averaged out along with the saturation inside the plume, leading to less restrictive time steps. A more restrictive time step due to the explicit calculation of the pseudo-residual saturation has only been observed for the local

pseudo-VE model. The correction resulting from that has been rarely necessary and has occurred only for the columns near the leading edge of the plume when the plume height was very small there (≈ 100 times smaller than the average height of the entire plume). However, small oscillations that can be observed in the saturation inside the plume of the local pseudo-VE model are attributed to the correction and initialization of columns at the leading edge of the plume. This can lead to slightly different plume heights and initial pseudo-residual saturations inside the columns at the leading edge of the plume at the start of segregation.

5.1. Comparison of Horizontal Plume Extent at $t=10 \times t_{seg}$

We take the horizontal plume extent as an indicator for accuracy. The horizontal plume extent refers to the horizontal distance from the injection point to the leading edge of the plume. The leading edge is defined as the location closest to the injection where the reconstructed nonwetting phase saturation is smaller than 1.0×10^{-6} . The comparison is done after a simulated time of $10 \times t_{seg}$, with the segregation time t_{seg} [T] calculated after Nordbotten and Dahle (2011). The segregation time can be used to estimate the time after which VE models are applicable and can be written as

$$t_{seg} = \frac{H\phi(1-s_{wr})\mu_w}{k_{r,w}kg(\rho_w - \rho_n)} \tag{26}$$

Practically, we choose the characteristic value for the relative permeability in (26) to be 1, which leads to an underestimation of the segregation time.

The horizontal plume extent for all VE models is plotted against the full multidimensional reference solutions in Figure 6. Both pseudo-VE models lead to a very good estimation of the horizontal plume extent. They compare well with the full multidimensional model for all cases, independent of the power law

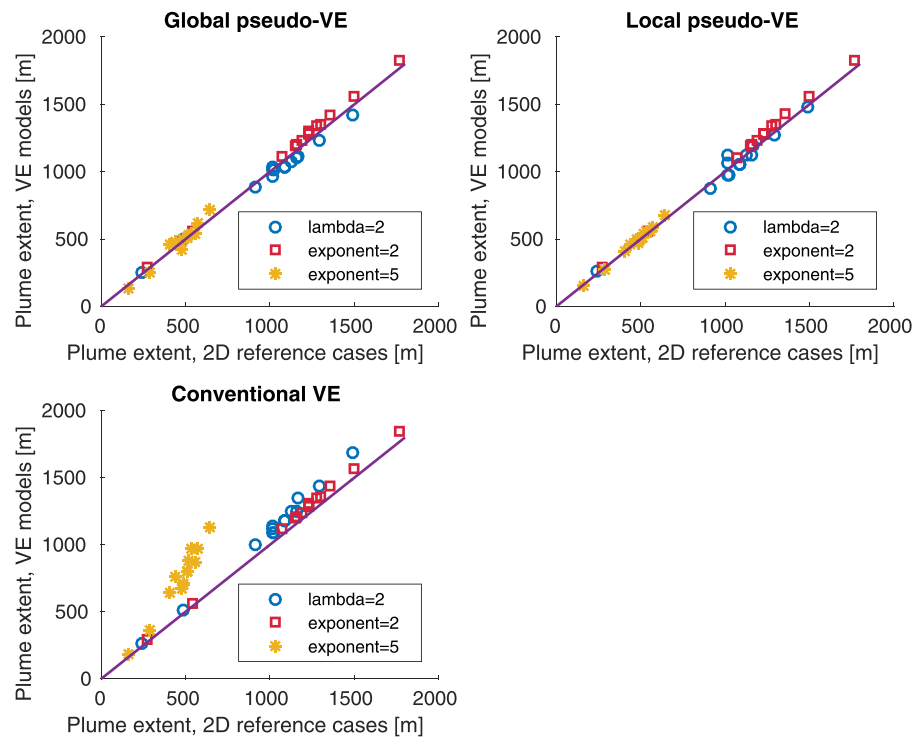


Figure 6. Horizontal plume extent for global pseudo-VE model, local pseudo-VE model, and conventional VE model over horizontal plume extent for full multidimensional reference. A perfect match to the reference solution is the purple line, dots above this line indicate overestimation of the horizontal plume extent and dots below this line indicate underestimation of the horizontal plume extent. The colors indicate the relative permeability-saturation relationship; Blue, Brooks-Corey law with $\lambda = 2$ (mixed case); red, power function with exponent 2 (low nonlinearity); and yellow, power function with exponent 5 (high nonlinearity).

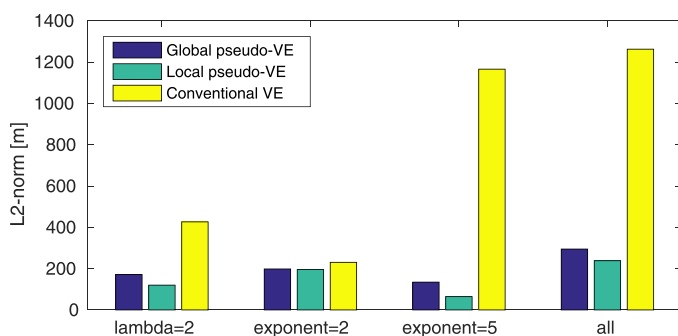


Figure 7. L2-norm for VE models for all test cases. The L2-norm is calculated as the square root of the sum of squares of differences in horizontal plume extent between the reference solution and the VE models.

nonlinearity of the relative permeability functions. Relative permeability functions with large exponents as well as the Brooks-Corey relationship with a parameter $\lambda = 2$ can be handled.

As expected, due to the nonlinear relative permeability functions used, the results show an overestimation of the horizontal plume extent for the conventional VE model for almost all test cases, in particular for the relative permeability cases with large exponents. This is because the conventional VE model does not reflect the slow gravity drainage since it assumes gravity segregation of both phases from the start. Especially in the case of relative permeability functions with large exponents, assuming gravity segregation from the beginning of simulation results in a higher coarse-scale relative permeability and consequently a much faster propagation of the front. The conventional VE model appears to give good results for cases with a large

permeability or a low injection rate as well. This is mostly due to the fact that the horizontal plume extent for these cases is smaller, leading to the dots in the figure to be closer to the reference line than for the other cases. However, the relative error (difference in horizontal plume extent in percentage of horizontal plume extent of the reference simulation) stays in the same range as for all other cases.

For relative permeability functions with low exponents the results of the pseudo-VE models recover the results of the conventional VE model, while all of them compare well with the results from the full multidimensional model. In cases with relative permeability functions with low exponents the assumption of instant segregation can be considered as more valid. Here both phases segregate faster because relative permeability does not reach very low values for medium wetting phase saturations. This is reflected in the pseudo-VE models by a faster segregation of the two phases, leading to similar results as for the conventional VE model. Additionally, for linear relative permeability functions, the coarse-scale relative permeability does not depend on the fine-scale saturation profile at all. Thus, a relative permeability function with low exponent (close to linear) results in less dependency of the coarse-scale relative permeability on a correct reconstruction of the saturation profile in the vertical direction. Accordingly, for these cases all VE models show generally satisfying agreement with the reference model.

The results indicate that including the segregation process in a simplified way (pseudo-VE model) gives saturation profiles in the vertical direction that are closer to the reference solution and results in a more correct coarse-scale relative permeability. Consequently, both pseudo-VE models greatly improve the results compared to the conventional VE model and thereby extend the applicability of VE models.

We also measure the difference between the three VE models and the reference solution using the L2-norm of the difference of the horizontal extent (Figure 7). The L2-norm is calculated as the square root of the sum of squares of differences in horizontal plume extent between the reference solutions and the three VE models. For the mixed cases and the cases with relative permeability functions with large exponents the L2-norm for both pseudo-VE models is significantly lower than for the conventional VE model. Only for the cases with low exponents the L2-norm is similar for all VE models. The global pseudo-VE model always shows a slightly higher L2-norm than the local pseudo-VE model, which is still significantly lower than for the conventional VE model.

5.2. Comparison of Horizontal Plume Extent at $t < 10 \times t_{seg}$

We analyze the horizontal plume extent for times closer to the estimated segregation time. This is done using case 1 and case 5 (large-permeability case with $k = 1,000$ mD) as examples, to show the influence of permeability. We use a Brooks-Corey relative permeability function with a parameter $\lambda = 2$ (mixed case) and relative permeability function with exponent 5 (highly nonlinear). The relative error is calculated as the difference between the horizontal plume extent resulting from the VE models and the reference solution, and given in percentage of the horizontal plume extent of the reference solution. The relative error is plotted over time normalized by the segregation time t_{seg} in Figure 8.

The global pseudo-VE model shows a less good agreement for early times. However, the results improve after approximately $5 \times t_{seg}$ for most cases, for both permeability functions. This is attributed to the global

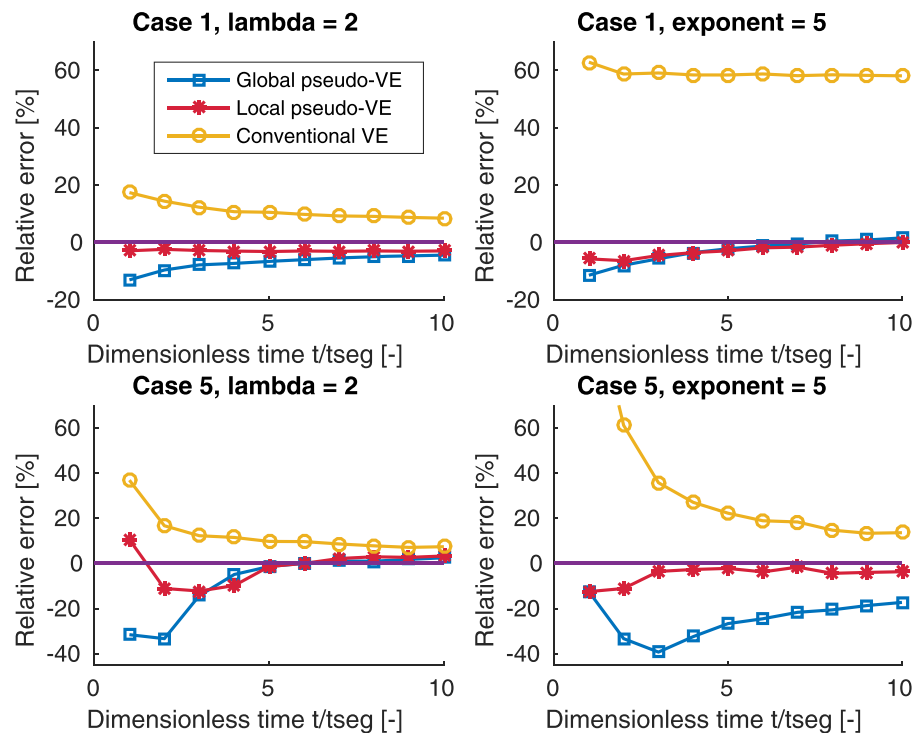


Figure 8. Relative error over dimensionless simulation time for global pseudo-VE model, local pseudo-VE model, and conventional VE model. First row, case 1; second row, case 5 (large-permeability case). First column, relative permeability function with Brooks-Corey $\lambda = 2$; second column, relative permeability function with exponent 5 (highly nonlinear). The relative error is calculated as the difference to the horizontal plume extent of the reference solution and given as the percentage of the horizontal plume extent of the reference solution.

pseudo-VE model being a very simple modification of the conventional VE model. It gives stable results but it neglects variations of the saturation inside the plume in the horizontal as well as vertical direction. During the fine-scale calculations we assume that the plume height is approximately the same everywhere to be able to calculate the drainage using an averaged plume height. This assumption does not hold for earlier simulation times when the horizontal plume shape has not developed yet. Consequently, this leads to the observed discrepancies between the reference solution and the global pseudo-VE model in earlier times and to a slower convergence toward the reference solution over time. The global pseudo-VE model manages to capture the horizontal plume extent well for later times, except for cases with large permeability and a relative permeability function with large exponent, where the horizontal plume extent is underestimated. This indicates that the correction of the global pseudo-VE model does not reflect the local processes equally well for all cases. However, the relative error in this case is in the range of the conventional VE model.

All results for the local pseudo-VE model show good agreement with the reference solution over all times, even times close to the segregation time. This holds for both the Brooks-Corey relative permeability function and the highly nonlinear relative permeability function. The local pseudo-VE model accounts for vertical fluxes by the explicit calculation of the pseudo-residual saturation in each single grid column. This way, the local pseudo-VE model includes variations of the saturation inside the plume along the horizontal direction. This is especially relevant for earlier times, during which the nonwetting plume exhibits large variations of the plume height along the horizontal direction, leading to different saturation values inside the plume. Consequently, the local pseudo-VE model leads to a very good approximation of the horizontal plume extent, even for relative permeability functions with large exponents and earlier times that are closer to the segregation time.

The conventional VE model overestimates the horizontal plume extent in all cases, especially for cases with relative permeability functions with large exponents. The solution of the conventional VE model seems to

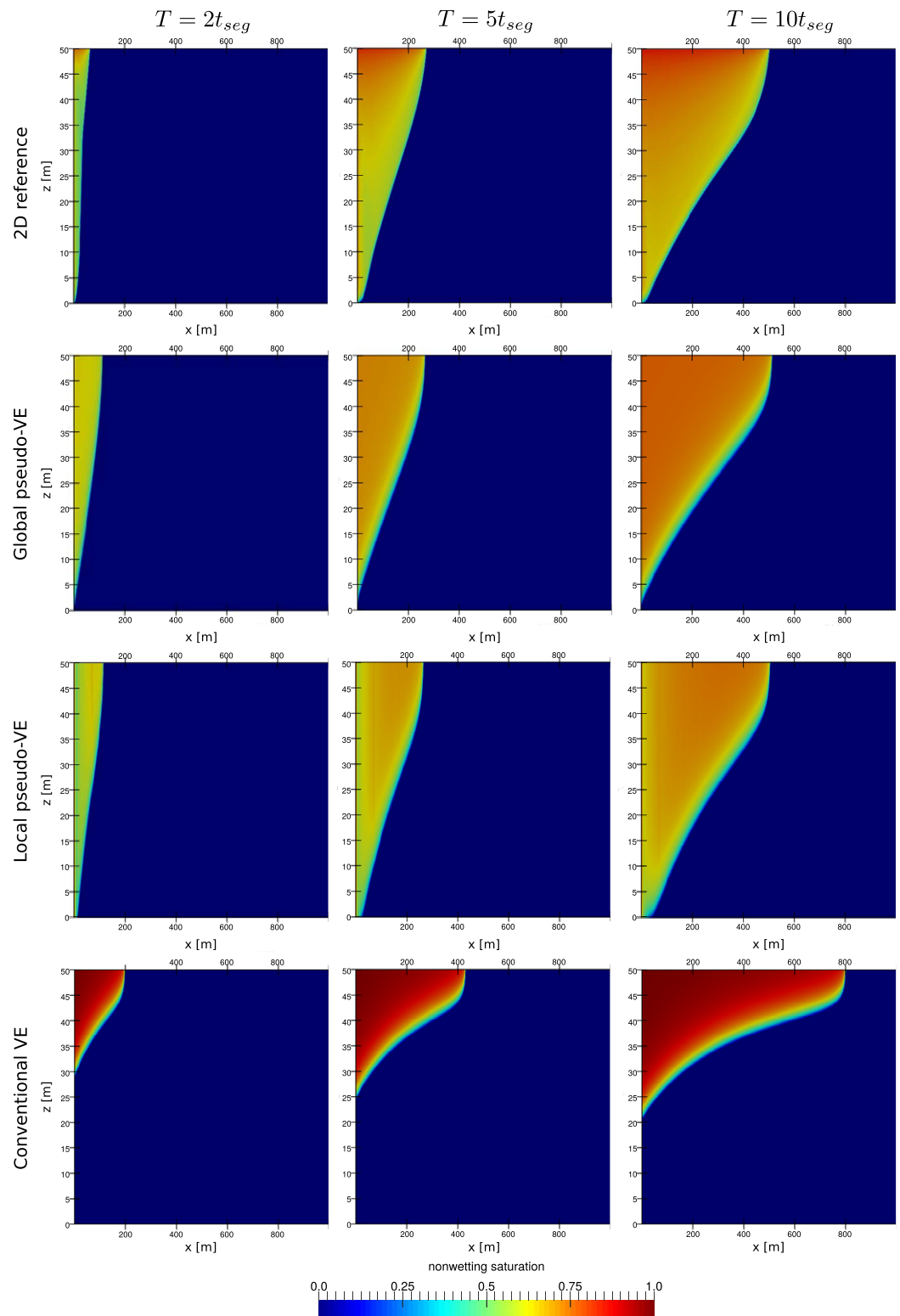


Figure 9. Gas distribution for 2-D reference, global pseudo-VE model, local pseudo-VE model, and conventional VE model for case 1 with highly nonlinear relative permeability function (exponent 5) for different time steps: $2 \times t_{seg}$, $5 \times t_{seg}$, and $10 \times t_{seg}$.

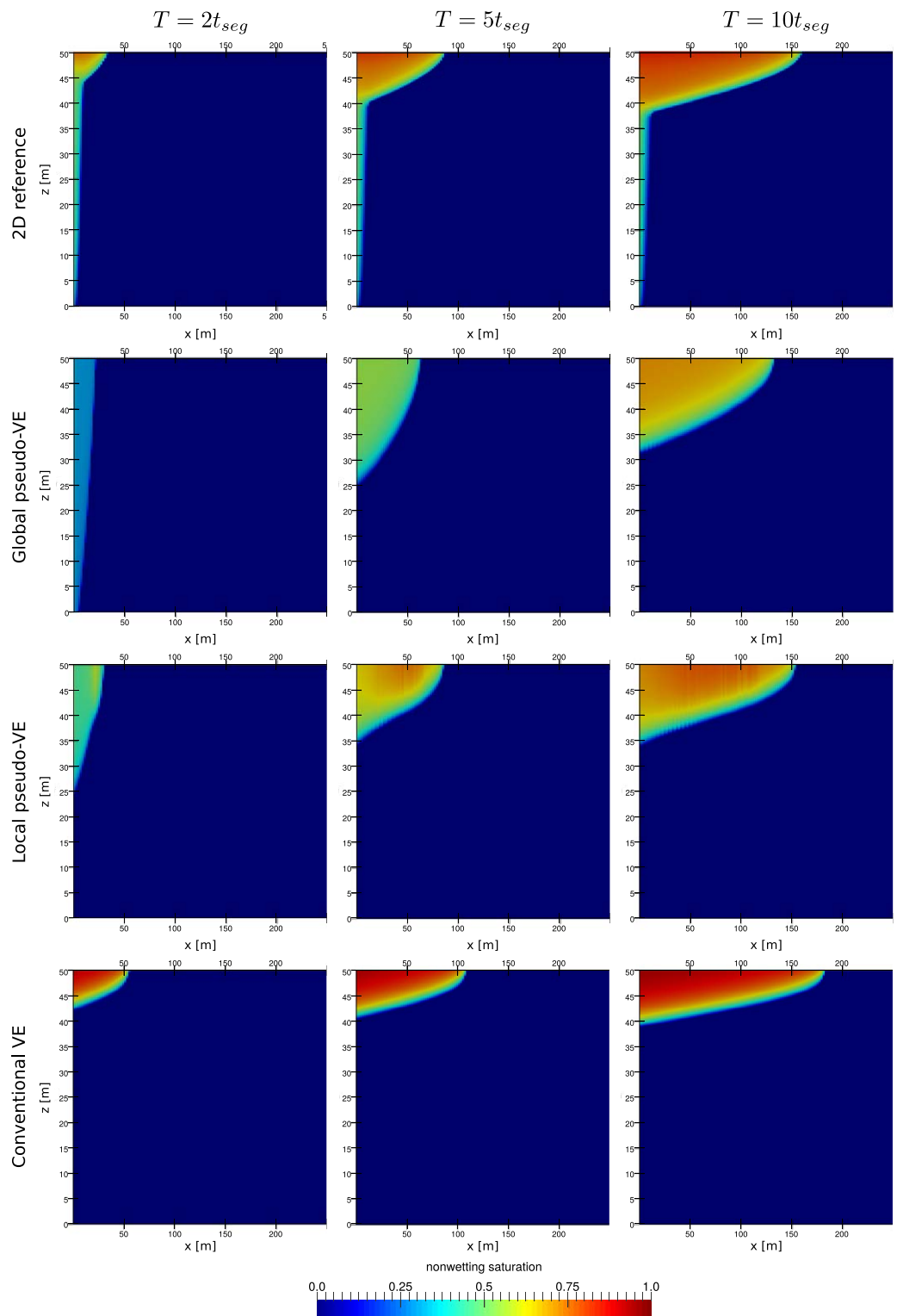


Figure 10. Gas distribution for 2-D reference, global pseudo-VE model, local pseudo-VE model, and conventional VE model for case 5 (large permeability $k = 1,000$ mD) with highly nonlinear relative permeability function (exponent 5) for different time steps: $2 \times t_{seg}$, $5 \times t_{seg}$, and $10 \times t_{seg}$.

approach the reference solution very slowly in general. This is again because instant gravity segregation is assumed and leads to incorrect saturation profiles in the vertical direction.

5.3. Comparison of Gas Distribution

We plot example saturation profiles for case 1 and case 5 (large-permeability case with $k = 1,000$ mD). We use a highly nonlinear relative permeability function (exponent 5). The results for the reference simulation and all VE models are shown in Figures 9 and 10 for three different time steps.

Case 1 shows that both the local pseudo-VE model and the global pseudo-VE model agree well with the reference solution over time. The variations in plume height along the horizontal direction are represented well. However, one can see a difference in saturation distribution within the plume. The reference solution shows a clear vertical gradient in saturation which is not represented by the VE models. As expected, the conventional VE model and the global pseudo-VE model have a uniform saturation inside the entire plume. The local pseudo-VE model shows variations along the horizontal direction, with lower saturation values around the injection area. The conventional VE model results in an incorrect plume shape with a very different saturation inside the plume compared to the reference solution. The plume is thinner, which leads to an overestimation of the horizontal plume extent.

Case 5 shows again a good agreement between reference solution and local pseudo-VE model. The global pseudo-VE model does not represent the plume height along the horizontal direction correctly for earlier times, which leads to an underestimation of the horizontal plume extent also for later times. The conventional VE model again shows an overall thinner plume and overestimation of the horizontal plume extent.

Compared to the multiscale dynamic reconstruction model in Guo et al. (2014) which produces results with a very high accuracy also in the vertical direction, both pseudo-VE models show a more simplified saturation profile in the vertical direction. This might have an impact especially for early simulation times and lead to less accurate results by the pseudo-VE models in comparison. Particularly the variations in the saturation profile in the vertical cannot be represented by the pseudo-VE models. In terms of computational effort, the multiscale dynamic reconstruction model relies on vertical fine-scale one-dimensional simulations inside each column. This requires gridding for the fine-scale simulation and storage of the data for the determination of the coarse-scale parameters by integration, which results in a more complex implementation and higher computational cost. The computational effort for the pseudo-VE models are similar to those for the conventional VE model, resulting in a faster computation compared to the multiscale dynamic reconstruction model. Thus, the pseudo-VE models can be seen as intermediate models between the conventional VE model and the multiscale dynamic reconstruction model in Guo et al. (2014). The decision of which model to take has to be done by weighing accuracy against computational speed based on the exact question of interest that is to be answered by the model.

6. Conclusions

In this paper, we developed a pseudo-VE model by casting it into a multiscale framework for VE models and treating the segregation process on the fine scale explicitly without having to rely on the VE assumption. The newly developed pseudo-VE model assumes a pseudo-segregated state with a pseudo-residual wetting phase saturation higher than the ultimate wetting phase saturation inside the plume, with the pseudo-residual saturation being continuously updated during the simulation. The pseudo-residual saturation can either be determined for the entire plume or for each column separately, leading to two versions of the pseudo-VE model.

The pseudo-VE models showed better (or equal) accuracy in predicting the gas plume extent compared to the conventional VE model throughout the range of aquifer parameters in our injection scenarios, in particular for relative permeability functions with large exponents. The local pseudo-VE model gives significantly improved results especially for earlier times of the simulation. The pseudo-VE models extend the applicability of VE models to cases with relative permeability functions with large exponents and shorter time scales, while fully maintaining the computational benefit of conventional VE models. As such, pseudo-VE models can provide a very efficient computational tool for dealing with practical cases of underground gas storage in which large domains, long simulation times and parameter uncertainty are major challenges.

Acknowledgments

Beatrix Becker is supported by a scholarship of the Landesgraduiertenförderung Baden-Württemberg at the University of Stuttgart. The code to produce the results presented here can be obtained from <https://git.iws.uni-stuttgart.de/dumux-pub/Becker2017a>.

References

- Ackermann, S., Beck, M., Becker, B., Class, H., Fetzer, T., Flemisch, B., . . . Weishaupt, K. (2017). *DuMu² 2.11.0*. Zenodo. <https://doi.org/10.5281/zenodo.439488>
- Bandilla, K. W., & Celia, M. A. (2017). Active pressure management through brine production for basin-wide deployment of geologic carbon sequestration. *International Journal of Greenhouse Gas Control*, *61*, 155–167. <https://doi.org/10.1016/j.ijggc.2017.03.030>
- Bandilla, K. W., Celia, M. A., Elliot, T. R., Person, M., Ellett, K. M., Rupp, J. A., . . . Zhang, Y. (2012). Modeling carbon sequestration in the Illinois basin using a vertically-integrated approach. *Computing and Visualization in Science*, *15*(1), 39–51.
- Bandilla, K. W., Celia, M. A., & Leister, E. (2014). Impact of model complexity on CO₂ plume modeling at Sleipner. *Energy Procedia*, *63*, 3405–3415.
- Celia, M., Bachu, S., Nordbotten, J., & Bandilla, K. (2015). Status of CO₂ storage in deep saline aquifers with emphasis on modeling approaches and practical simulations. *Water Resources Research*, *51*, 6846–6892. <https://doi.org/10.1002/2015WR017609>
- Class, H., A., Ebigbo, R., Helmig, H. K., Dahle, J. M., Nordbotten, M. A., Celia, P., . . . Wei, L. (2009). A benchmark study on problems related to CO₂ storage in geologic formations. *Computational Geosciences*, *13*(4), 409.
- Courant, R., Friedrichs, K., & Lewy, H. (1928). Über die partiellen Differenzengleichungen der mathematischen Physik. *Mathematische Annalen*, *100*, 32–74. <https://doi.org/10.1007/BF01448839>
- Court, B., Bandilla, K. W., Celia, M. A., Janzen, A. J., Dobossy, M., & Nordbotten, J. M. (2012). Applicability of vertical-equilibrium and sharp-interface assumptions in CO₂ sequestration modeling. *International Journal of Greenhouse Gas Control*, *10*, 134–147.
- Dentz, M., & Tartakovsky, D. M. (2009). Abrupt-interface solution for carbon dioxide injection into porous media. *Transport in Porous Media*, *79*(1), 15.
- Ewing, R. P., Ghanbarian, B., & Hunt, A. G. (2015). Gradients and assumptions affect interpretation of laboratory-measured gas-phase transport. *Soil Science Society of America Journal*, *79*(4), 1018–1029.
- Flemisch, B., Darcis, M., Erbertseder, K., Faigle, B., Lauser, A., Mosthaf, K., . . . Helmig, R. (2011). DuMu²: DUNE for multi-(phase, component, scale, physics, . . .) flow and transport in porous media. *Advances in Water Resources*, *34*(9), 1102–1112.
- Gasda, S. E., Nordbotten, J. M., & Celia, M. A. (2012). Application of simplified models to CO₂ migration and immobilization in large-scale geological systems. *International Journal of Greenhouse Gas Control*, *9*, 72–84.
- Golding, M. J., Neufeld, J. A., Hesse, M. A., & Huppert, H. E. (2011). Two-phase gravity currents in porous media. *Journal of Fluid Mechanics*, *678*, 248–270.
- Guo, B., Bandilla, K. W., Doster, F., Keilegavlen, E., & Celia, M. A. (2014). A vertically integrated model with vertical dynamics for CO₂ storage. *Water Resources Research*, *50*, 6269–6284. <https://doi.org/10.1002/2013WR015215>
- Guo, B., Zheng, Z., Celia, M. A., & Stone, H. A. (2016). Axisymmetric flows from fluid injection into a confined porous medium. *Physics of Fluids*, *28*(2), 022107.
- Hesse, M., Tchelepi, H., Cantwel, B., & Orr, F. (2007). Gravity currents in horizontal porous layers: Transition from early to late self-similarity. *Journal of Fluid Mechanics*, *577*, 363–383.
- Hunt, A., Ewing, R., & Ghanbarian-Alavijeh, B. (2013). *Percolation theory for flow in porous media, Lecture Notes in Physics* (Vol. 880). Berlin, Germany: Springer.
- Huppert, H. E., & Woods, A. W. (1995). Gravity-driven flows in porous layers. *Journal of Fluid Mechanics*, *292*(1), 55.
- Juanes, R., MacMinn, C. W., & Szulczewski, M. L. (2010). The footprint of the CO₂ plume during carbon dioxide storage in saline aquifers: Storage efficiency for capillary trapping at the basin scale. *Transport in Porous Media*, *82*(1), 19–30.
- Lake, L. W. (1989). *Enhanced oil recovery*. Englewood Cliffs, NJ: Prentice Hall.
- Ligaarden, I., & Nilsen, H. (2010). Numerical aspects of using vertical equilibrium models for simulating CO₂ sequestration. In *ECMOR XII-12th European conference on the mathematics of oil recovery*. Oxford, UK: EAGE.
- Lyle, S., Huppert, H. E., Hallworth, M., Bickle, M., & Chadwick, A. (2005). Axisymmetric gravity currents in a porous medium. *Journal of Fluid Mechanics*, *543*, 293–302.
- Metz, B., Davidson, O., Coninck, H. D., Loos, M., & Meyer, L. (2005). *IPCC special report on carbon dioxide capture and storage* (technical report). Geneva, Switzerland: Intergovernmental Panel on Climate Change, Working Group III.
- Mignard, D., Wilkinson, M., & Amid, A. (2016). Seasonal storage of hydrogen in a depleted natural gas reservoir. *International Journal of Hydrogen Energy*, *41*(12), 5549–5558. <https://doi.org/10.1016/j.ijhydene.2016.02.036>
- Nilsen, H. M., Herrera, P. A., Ashraf, M., Ligaarden, I., Iding, M., Hermanrud, C., . . . Keilegavlen, E. (2011). Field-case simulation of CO₂-plume migration using vertical-equilibrium models. *Energy Procedia*, *4*, 3801–3808.
- Nordbotten, J., B., Flemisch, S., Gasda, H., Nilsen, Y., Fan, G., Pickup, B., . . . Pruess, K. (2012). Uncertainties in practical simulation of CO₂ storage. *International Journal of Greenhouse Gas Control*, *9*, 234–242.
- Nordbotten, J. M., & Celia, M. A. (2006). Similarity solutions for fluid injection into confined aquifers. *Journal of Fluid Mechanics*, *561*, 307–327.
- Nordbotten, J. M., & Celia, M. A. (2011). *Geological storage of CO₂: Modeling approaches for large-scale simulation*. Hoboken, NJ: John Wiley.
- Nordbotten, J. M., & Dahle, H. K. (2011). Impact of the capillary fringe in vertically integrated models for CO₂ storage. *Water Resources Research*, *47*, W02537. <https://doi.org/10.1029/2009WR008958>
- Oldenburg, C. M., & Pan, L. (2013). Porous media compressed-air energy storage (PM-CAES): Theory and simulation of the coupled well-bore-reservoir system. *Transport in Porous Media*, *97*(2), 201–221.
- Pegler, S. S., Huppert, H. E., & Neufeld, J. A. (2014). Fluid injection into a confined porous layer. *Journal of Fluid Mechanics*, *745*, 592–620.
- Person, M., Banerjee, A., Rupp, J., Medina, C., Lichtner, P., Gable, C., . . . Bense, V. (2010). Assessment of basin-scale hydrologic impacts of CO₂ sequestration, Illinois basin. *International Journal of Greenhouse Gas Control*, *4*(5), 840–854.
- Pfeiffer, W. T., Beyer, C., & Bauer, S. (2017). Hydrogen storage in a heterogeneous sandstone formation: Dimensioning and induced hydraulic effects. *Petroleum Geoscience*, *23*, <https://doi.org/10.1144/petgeo2016-050>
- Swickrath, M. J., Mishra, S., & Ravi Ganesh, P. (2016). An evaluation of sharp interface models for CO₂-brine displacement in aquifers. *Ground Water*, *54*(3), 336–344. <https://doi.org/10.1111/gwat.12366>
- Yortsos, Y. (1995). A theoretical analysis of vertical flow equilibrium. *Transport in Porous Media*, *18*(2), 107–129.
- Zheng, Z., Guo, B., Christov, I. C., Celia, M. A., & Stone, H. A. (2015). Flow regimes for fluid injection into a confined porous medium. *Journal of Fluid Mechanics*, *767*, 881–909.